

See discussions, stats, and author profiles for this publication at: <https://www.researchgate.net/publication/231400843>

# AM1 and PM3 calculations of the potential energy surfaces for hydroxymethyl radical reactions with nitric oxide and nitrogen dioxide

ARTICLE *in* THE JOURNAL OF PHYSICAL CHEMISTRY · JUNE 1991

Impact Factor: 2.78 · DOI: 10.1021/j100166a034

---

CITATIONS

7

---

READS

26

2 AUTHORS, INCLUDING:



George C Shields

Bucknell University

96 PUBLICATIONS 3,987 CITATIONS

SEE PROFILE

is lost due to the smaller ion-dipole interaction (dipole moment of  $\text{C}_2\text{H}_5\text{OC}_2\text{H}_5 = 1.15 \text{ D}$ ), as compared to  $\text{CH}_3\text{CHO}$  ( $2.69 \text{ D}$ ) and  $\text{C}_2\text{H}_5\text{OH}$  ( $1.69 \text{ D}$ ).<sup>40</sup>

**b.  $(\text{DEE})_n^+$  and  $(\text{DEE})_n\text{H}^+$ .** Experimentally we find that one  $\text{C}_2\text{H}_4$  molecule is eliminated in a few microsecond time window from the protonated monomer ion  $(\text{DEE})\text{H}^+$  as demonstrated in Figure 8. However, loss of  $\text{C}_2\text{H}_5$  from  $(\text{DEE})_2^+$  is observed, which suggests that the unprotonated dimer is very strongly bonded (otherwise loss of  $\text{C}_2\text{H}_5\text{OC}_2\text{H}_5$  or  $\text{C}_2\text{H}_5\text{OC}_2\text{H}_4$  would be seen). The following energetic consideration provides a satisfactory explanation.

The binding energy of  $\text{DEEH}^+\cdot\text{DEE}$  is measured<sup>34</sup> to be  $1.2 \text{ eV}$ . The value for  $(\text{C}_2\text{H}_5\text{OC}_2\text{H}_4)\text{H}^+\cdot\text{DEE}$  or  $\text{DEEH}^+\cdot(\text{C}_2\text{H}_5\text{OC}_2\text{H}_4)$  should be of comparable magnitude since similar hydrogen bonding is present. The calculated<sup>33</sup> heat of formation of  $\text{CH}_3\text{CH}_2\text{O}(\text{H})\text{CHCH}_3^+$  is  $626.5 \text{ kJ/mol}$  (the experimental value is not available). For  $\text{CH}_3\text{CHOH}^+$  and  $\text{CH}_3\text{CH}_2^+$ , the values are known<sup>35</sup> to be  $583 \text{ kJ/mol}$  and  $118 \text{ kJ/mol}$ , respectively. Hence, the following reaction



is endothermic by  $74.5 \text{ kJ/mol}$  or  $0.71 \text{ eV}$ , which is less than the hydrogen-bond energy (about  $1.2 \text{ eV}$ ) of the dimer ion.

(40) Nelson, R. D., Jr.; Lide, D. R., Jr.; Maryott, A. A. Selected Values of Electric Dipole Moments for Molecules in the Gas Phase. NSRDS-NBS 10; NBS: Washington, D.C., 1967.

As for  $(\text{DEE})_2\text{H}^+\cdot\text{DEE}$ , even though the binding energy is not known, the value is expected to be much smaller than  $1.2 \text{ eV}$  due to the complete hydrogen-bonding solvation shell formation at  $(\text{DEE})_2\text{H}^+$ . The binding energy of cluster ion  $(\text{CH}_3\text{OCH}_3)_2\text{H}^+\cdot\text{CH}_3\text{OCH}_3$  is measured to be  $0.40 \text{ eV}$ , and that of  $(\text{C}_2\text{H}_5\text{OC}_2\text{H}_5)_2\text{H}^+\cdot\text{C}_2\text{H}_5\text{OC}_2\text{H}_5$  should be of comparable magnitude, which is smaller than the energy required for reaction 20. Our observation of  $\text{C}_2\text{H}_5\text{OC}_2\text{H}_4$  loss for  $n = 3$  and  $\text{C}_2\text{H}_5\text{O}\cdot\text{C}_2\text{H}_5$  loss for  $n = 4$  is consistent with these thermochemical values and the general expectation that the reaction pathways are based on the energetics.

#### IV. Conclusion

A number of chemical reactions take place upon multiphoton ionization of neutral dimethyl and diethyl ether clusters. Inter-molecular proton-transfer reactions dominate in both cases, as evidenced by the fact that protonated cluster ions are the most abundant species. An intramolecular hydrogen-transfer reaction is responsible for the unique stability of unprotonated diethyl ether dimer ion. It is observed that the presence of water molecules greatly suppresses reactions leading to product  $(\text{CH}_3\text{OCH}_3)_n\text{CH}_3\text{OH}_2^+$ , but formation of  $(\text{C}_2\text{H}_5\text{OC}_2\text{H}_5)_n\text{C}_2\text{H}_5\text{OH}_2^+$  is not influenced. These findings can be understood on the basis of different reaction mechanisms.

**Acknowledgment.** Support by the U.S. Department of Energy, Grant No. DE-FG02-88-ER60668, is gratefully acknowledged.

## AM1 and PM3 Calculations of the Potential Energy Surfaces for $\text{CH}_2\text{OH}$ Reactions with $\text{NO}$ and $\text{NO}_2$

Georgia H. Kalkanis and George C. Shields\*

Department of Chemistry, Lake Forest College, Lake Forest, Illinois 60045 (Received: July 27, 1990)

The AM1 and PM3 molecular orbital methods have been utilized to investigate the reactions of  $\text{CH}_2\text{OH}$  with  $\text{NO}$  and  $\text{NO}_2$ . PM3 and AM1 calculated heats of formation differ from experimental values by  $8.6$  and  $18.8 \text{ kcal mol}^{-1}$ , respectively. The dominant reaction of  $\text{CH}_2\text{OH}$  with  $\text{NO}$  is predicted to produce the adduct  $\text{HOCH}_2\text{NO}$ , supporting the hypothesis of Pagsberg, Munk, Anastasi, and Simpson. Calculated activation energies for the  $\text{NO}_2$  system predict the formation of the adducts  $\text{HOCH}_2\text{NO}_2$  and  $\text{HOCH}_2\text{ONO}$ . In addition, the PM3 calculations predict that the abstraction reaction producing  $\text{CH}_2\text{O}$  and  $\text{HNO}_2$  is more likely than one producing  $\text{CH}_2\text{O}$  and  $\text{HONO}$  from reactions of  $\text{CH}_2\text{OH}$  with  $\text{NO}_2$ .

#### Introduction

The hydroxymethyl and methoxy radicals are important intermediates in the combustion of methanol.<sup>1</sup> There have been many studies concerning the methoxy radical but relatively few on its isomer. Most of the previous studies of the hydroxymethyl radical,  $\text{CH}_2\text{OH}$ , have concerned the kinetics of reactions involving  $\text{O}_2$ .<sup>2-6</sup> The ultraviolet absorption spectrum of  $\text{CH}_2\text{OH}$  has been reported<sup>7,8</sup> and used to monitor the kinetic behavior of this radical in reactions with  $\text{O}_2$ ,  $\text{NO}$ , and  $\text{NO}_2$  at room temperature and  $1 \text{ atm}$  pressure.<sup>9</sup> The present work uses semiempirical molecular orbital methods to calculate the activation energy barriers and

energetics for reactions of  $\text{CH}_2\text{OH}$  with  $\text{NO}$  and  $\text{NO}_2$ .

These methods have been developed and used to study the molecular structure and reactivities of molecules, ions, and radicals.<sup>10-13</sup> The MNDO method was parametrized using 34 molecules for the C-H-N-O set<sup>11</sup> while for AM1 approximately 100 molecules were used for this parametrization.<sup>12</sup> Several hundred molecules were used in the PM3 optimization,<sup>13</sup> as Stewart optimized PM3 in a cyclic fashion. For the PM3 method, any compound for which the properties were badly reproduced with a particular parameter set was included in the next stage of the optimization. This procedure for optimizing parameters consequently minimized errors for systems that initially had large deviations from experimental values. Dewar has shown that the mean absolute errors for neutral radicals are approximately  $2.5 \text{ kcal mol}^{-1}$  higher than for neutral molecules for the MNDO method.<sup>11</sup> The 14 radicals studied by MNDO were systematically predicted to be somewhat too stable.<sup>11</sup> This deficiency was removed in the AM1 method, with the notable exceptions of  $\text{NO}$

(1) Warnatz, J. In *Combustion Chemistry*; Gardiner, W. C., Jr., Ed.; Springer-Verlag: New York, 1984.

(2) Radford, H. E. *Chem. Phys. Lett.* **1980**, *71*, 195.

(3) Wang, W. C.; Suto, M.; Lee, L. C. *J. Chem. Phys.* **1984**, *81*, 3122.

(4) Grotheer, H. H.; Rieker, G.; Meier, U.; Just, T. *Ber. Bunsen-Ges. Phys. Chem.* **1985**, *89*, 187.

(5) Dobe, S.; Temps, F.; Bohland, T.; Wagner, H. G. *Z. Naturforsch.* **1985**, *40A*, 1289.

(6) Payne, W. A.; Brunning, J.; Mitchell, M. B.; Stief, L. *J. Int. J. Chem. Kinet.* **1988**, *20*, 63.

(7) Pagsberg, P.; Munk, J.; Sillesen, A.; Anastasi, C. *Chem. Phys. Lett.* **1988**, *146*, 375.

(8) Rettrup, S.; Pagsberg, P.; Anastasi, C. *Chem. Phys.* **1988**, *122*, 45.

(9) Pagsberg, P.; Munk, J.; Anastasi, C.; Simpson, V. J. *J. Phys. Chem.* **1989**, *93*, 5162.

(10) Bingham, R. C.; Dewar, M. J. S.; Lo, D. H. *J. Am. Chem. Soc.* **1975**, *97*, 1285, 1294, 1302, 1307.

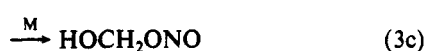
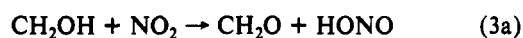
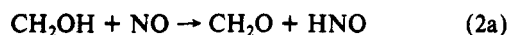
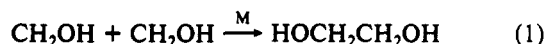
(11) Dewar, M. J. S.; Thiel, W. *J. Am. Chem. Soc.* **1977**, *99*, 4899, 4907.

(12) Dewar, M. J. S.; Zoebisch, E. G.; Healy, E. F.; Stewart, J. J. P. *J. Am. Chem. Soc.* **1985**, *107*, 3902.

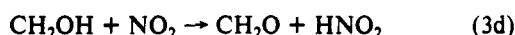
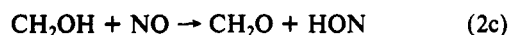
(13) Stewart, J. J. P. *J. Comput. Chem.* **1989**, *10*, 209, 221.

and  $\text{NO}_2$ .<sup>12</sup> The new parametrization used to generate the PM3 method<sup>13</sup> has reduced the overall error between heats of formation for neutral radicals and neutral molecules even further. Extensive calculations of reactions of radicals have not yet been performed with the PM3 method. In this paper, results are compared with pulse radiolysis/kinetic analysis experiments<sup>9</sup> and other experimental values.

Pagsberg et al.<sup>9</sup> reacted  $\text{CH}_2\text{OH}$  with various target molecules and used the ultraviolet absorption spectrum of  $\text{CH}_2\text{OH}$  to monitor its decomposition. They proposed the following reaction mechanisms to account for the varying reactivity of  $\text{CH}_2\text{OH}$  with NO and  $\text{NO}_2$ :



In this work the following reactions have also been considered:



The goal of this work is to compare and contrast the experimental information with results of quantum mechanical calculations in order to gain further insight into reactions of  $\text{CH}_2\text{OH}$  with NO and  $\text{NO}_2$ .

## Method

In this investigation the semiempirical molecular orbital programs developed by Dewar and co-workers<sup>10-13</sup> have been employed to calculate the products and transition-state structures for reactions of  $\text{CH}_2\text{OH}$  with NO and  $\text{NO}_2$ . MINDO/3, based on the INDO approximation, was the first truly successful semiempirical molecular orbital program.<sup>10,14</sup> In this quantum mechanical method, valence electrons are assumed to move in a fixed core of nuclei and inner-shell electrons and are treated by using a minimum basis set simplified by neglecting certain electron repulsion integrals involving differential overlap. The remaining integrals are then equated to functions containing numeric parameters that have been adjusted to fit experimental data. MINDO/3 has been very effective in studies of hydrocarbons but is not as good for molecules containing heteroatoms. This problem is a consequence of the neglect of one-center overlap in the INDO approximation on which MINDO/3 is based.<sup>10</sup>

MNDO was developed on the NDDO approximation, and the main improvements over MINDO/3 were for aromatic compounds, molecules with triple bonds, three-membered rings, and molecules with N-N bonds.<sup>11</sup> These improvements have been attributed to the inclusion of directional effects in the two-center MNDO electron-electron repulsions and core-electron attractions. Dewar's group next developed AM1, a new parametrization based on the NDDO approximation, with a modified core repulsion function. This second generation modified NDDO method represented an improvement over MNDO, with the main benefit being more accurate estimates of activation energies for reactions.<sup>12</sup> Recently, a third generation modified NDDO molecular model, PM3, has been developed<sup>13</sup> by using a new optimization procedure for quickly determining atomic parameters from experimental reference data. With this method the average difference between calculated heats of formation and experimental values for 657

TABLE I: Calculated and Experimental Heats of Formation for Reactants ( $\Delta H_f^\circ$ ) and Potential Products in Reactions of Gaseous  $\text{CH}_2\text{OH}$  with NO,  $\text{NO}_2$ , and  $\text{CH}_2\text{OH}$

molecule	$\Delta H_f^\circ$ , kcal/mol			ref
	AM1	PM3	exp	
$\text{CH}_2\text{OH}$	-26.5	-23.5	-6.2	16
NO	1.2	14.7	21.6	11
$\text{NO}_2$	-15.0	-1.0	7.91	17
$\text{CH}_2\text{O}$	-31.5	-34.1	-26.0	18
HNO	2.2	13.8	23.8	17
HON	42.4	49.0		
$\text{HOCH}_2\text{NO}$	-45.2	-33.8		
$\text{HOCH}_2\text{ON}$	-8.4	4.8		
$\text{HNO}_2$	-13.6	-17.6		
HONO	-39.4	-14.9	-18.8	17
$\text{HOCH}_2\text{NO}_2$	-57.1	-55.8		
$\text{HOCH}_2\text{ONO}$	-91.6	-53.2		
$\text{HOCH}_2\text{CH}_2\text{OH}$	-111.4	-98.6	-93.05, -92.6	19, 20

compounds is 7.8 kcal/mol, as compared to 12.7 and 13.9 kcal/mol for AM1 and MNDO, respectively.<sup>13</sup> PM3 is particularly better than the prior methods for heat of formation calculations of hypervalent species.

In this study MOPAC 5.0 software<sup>15</sup> has been utilized to calculate the heats of formation ( $\Delta H_f^\circ$ ) and geometries for  $\text{CH}_2\text{OH}$ , NO, and  $\text{NO}_2$ . Fully optimized geometries have also been obtained for the products and transition states formed in the reactions of the hydroxymethyl radical with NO and  $\text{NO}_2$ . No assumptions were made concerning the geometry of the transition state. The transition state both corresponds to a stationary point on the potential energy surface and is a saddle point (not the top of a hill). Saddle points are calculated within MOPAC by the procedure of McIver and Komornicki, by calculating and diagonalizing the Hessian matrix, or by Bartel's method, a nonlinear least-squares gradient minimization routine.<sup>15</sup> The force constant matrix at the transition state must have one and only one negative value in order to characterize the geometry as a saddle point. Restricted Hartree-Fock calculations were performed using both the AM1 and PM3 Hamiltonians. The criteria for terminating all optimizations was increased 100-fold over the normal MOPAC limits, and vibrational frequencies were calculated for each species to characterize ground and transition states. All calculations were carried out on a microVAX 3400 at Lake Forest College.

## Results and Discussion

Results of MOPAC calculations using the AM1 and PM3 Hamiltonians are presented in Tables I and II. Table I lists calculated and experimental heats of formation for reactants and potential products which would be formed by reactions 1-3. It should be noted that in most cases the PM3 calculations are closer to the experimental heats of formation than the AM1 values. Indeed, for the seven molecules where experimental numbers are available, the average error in the heats of formation are 18.8 kcal mol<sup>-1</sup> for AM1 and 8.6 kcal mol<sup>-1</sup> for PM3.

The major differences between the AM1 and PM3 calculated values are for NO,  $\text{NO}_2$ , HNO,  $\text{HOCH}_2\text{NO}$ ,  $\text{HOCH}_2\text{ON}$ , and  $\text{HOCH}_2\text{CH}_2\text{OH}$ , where the difference between the two methods ranges from 11 to 15 kcal mol<sup>-1</sup> and for HONO and  $\text{HOCH}_2\text{ONO}$ , where the methods differ by approximately 24 and 38 kcal mol<sup>-1</sup>, respectively. For every one of these species the PM3 calculation yields a higher energy value than the corresponding

(15) Stewart, J. J. P. QCPE 455. Available from Indiana University, Department of Chemistry, Bloomington, IN.

(16) McMillen, D. F.; Golden, D. M. *Annu. Rev. Phys. Chem.* **1982**, *33*, 493-532.

(17) Stull, D. R.; Westrum, E. F., Jr.; Sinke, G. C. *The Chemical Thermodynamics of Organic Compounds*; John Wiley and Sons: New York, 1982.

(18) Stull, D. R.; Prophet, H. In *JANAF Thermochemical Tables*; National Bureau of Standards: Washington, DC, 1971.

(19) Cox, J. D.; Pilcher, G. *Thermochemistry of Organic and Organometallic Compounds*; Academic Press: New York, 1970.

(20) Lias, S. G.; Bartmess, J. E.; Liebman, J. F.; Holmes, J. L.; Levin, R. D.; Mallard, W. G. Gas-Phase Ion and Neutral Thermochemistry. *J. Phys. Chem. Ref. Data* **1988**, *17* (Suppl. 1).

(14) Pilar, F. L. *Elementary Quantum Chemistry*; McGraw-Hill: New York, 1990.

TABLE II: Calculated Heats of Formation for the Transition-State Structures Formed from Reactions of CH<sub>2</sub>OH with NO, NO<sub>2</sub>, and CH<sub>2</sub>OH and Calculated Activation Energy Barriers and Overall Enthalpy Change for Reactions of CH<sub>2</sub>OH<sup>b</sup>

reaction	$\Delta H_f^\circ$ <sup>298</sup>		activation energy		enthalpy change	
	AM1	PM3	AM1	PM3	AM1	PM3
1. CH <sub>2</sub> OH + CH <sub>2</sub> OH → HOCH <sub>2</sub> CH <sub>2</sub> OH	-110.3	-97.6	-57.3	-50.6	-58.3	-51.0
2a. CH <sub>2</sub> OH + NO → CH <sub>2</sub> O + HNO	13.2	30.1	38.5	38.9	-4.0	-11.5
2b. CH <sub>2</sub> OH + NO → HOCH <sub>2</sub> NO	-44.1	-31.4	-18.8	-22.6	-19.9	-25.0
2c. CH <sub>2</sub> OH + NO → CH <sub>2</sub> O + HON	45.1	<sup>a</sup>	70.4	<sup>a</sup>	36.2	23.7
2d. CH <sub>2</sub> OH + NO → HOCH <sub>2</sub> ON	-6.4	6.8	18.9	15.6	16.9	13.6
3a. CH <sub>2</sub> OH + NO <sub>2</sub> → CH <sub>2</sub> O + HONO	-42.2	-8.4	-3.3	16.1	-30.4	-24.5
3b. CH <sub>2</sub> OH + NO <sub>2</sub> → HOCH <sub>2</sub> NO <sub>2</sub>	-35.5	-22.7	5.0	1.8	-16.6	-31.3
3c. CH <sub>2</sub> OH + NO <sub>2</sub> → HOCH <sub>2</sub> ONO	-43.8	-18.3	-3.3	6.2	-51.1	-28.7
3d. CH <sub>2</sub> OH + NO <sub>2</sub> → CH <sub>2</sub> O + HNO <sub>2</sub>	-51.0	-53.5	-10.5	-29.0	-4.6	-27.2

<sup>a</sup> Unable to locate the saddle point for reaction 2c using PM3. <sup>b</sup> All values in kcal/mol.

AM1 number, bringing the semiempirical calculations closer to the experimental results. For HONO, the AM1 calculation gives a heat of formation of -39.4 kcal mol<sup>-1</sup> while the PM3 calculation results in a heat of -14.9 kcal mol<sup>-1</sup>. This result, where the PM3 number is quite close to the experimental value of -18.8 kcal mol<sup>-1</sup>, illustrates how the improved parametrization routine used to establish the PM3 Hamiltonian<sup>13</sup> minimizes errors for systems where AM1 gives large deviations from experimental values. Table I shows similar behavior for NO, NO<sub>2</sub>, and HNO, where the AM1 values deviate from experiment by 20–25 kcal mol<sup>-1</sup> and the corresponding PM3 values deviate by approximately 7–10 kcal mol<sup>-1</sup>.

Historically, Dewar's semiempirical methods<sup>10–12</sup> have reproduced heats of formation for diatomic and triatomic molecules rather poorly. This was not considered a major problem since the object of these methods has been to reproduce the chemistry of a wide range of organic compounds. The great success of the MINDO/3 and MNDO methods results from the fact that they reproduce molecular properties fairly accurately for a wide range of molecules, most of which were not included in the initial parametrization of the methods. While one could develop a semiempirical method that could accurately reproduce the heats of formation for, say, NO, NO<sub>2</sub>, and HNO, the method would have limited utility to chemists in general if it could not successfully handle other classes of compounds. It should be noted that the latest MNDO method, PM3, has lowered the error in heats of formation for both large molecules and smaller diatomics and triatomics.

It is interesting to compare heats of formation calculated by MOPAC with those computed by using Benson's rules.<sup>21,22</sup> Benson tabulated the heat of formation contribution for different bonds, so that the heat of formation for an entire molecule could be estimated by summing the contributions of all of the bonds in the molecule. Values of  $\Delta H_f^\circ$  are generally estimated within a few kcal mol<sup>-1</sup> although large errors result for compounds containing very electronegative groups such as NO<sub>2</sub>,<sup>22</sup> a result attributed to the high polarity of the NO<sub>2</sub> group.<sup>21</sup> No contribution for the N–O bond to the heat of formation is given by Benson, although the (NO)–O bond is listed with a value of 9.0 kcal mol<sup>-1</sup>. Thus, the heats of formation for NO, HNO, HON, HOCH<sub>2</sub>NO, and HOCH<sub>2</sub>ON cannot be determined by using Benson's rules. Heats of formation calculated by using Benson's rules for CH<sub>2</sub>OH, NO<sub>2</sub>, CH<sub>2</sub>O, HNO<sub>2</sub>, HONO, HOCH<sub>2</sub>NO<sub>2</sub>, HOCH<sub>2</sub>ONO, and HOCH<sub>2</sub>CH<sub>2</sub>OH are -46.66, 9, -19.66, 6.4, -18, -28.36, -49.66, and -90.59 kcal mol<sup>-1</sup>, respectively. Comparison of these estimates with the data in Table I shows that NO<sub>2</sub>, HONO, and HOCH<sub>2</sub>CH<sub>2</sub>OH are described accurately with Benson's rules while CH<sub>2</sub>OH and CH<sub>2</sub>O are not.

Transition-state heats of formation for each reaction are listed in Table II. A comparison of the energies for reactants, products, and transition states for each possible reaction is shown with the help of figures. Figures 1–4 depict the energetics of the reactions of CH<sub>2</sub>OH with NO and NO<sub>2</sub>, for both the AM1 and PM3

calculations. The sum of the calculated heats of formation for the reactants is plotted on the left-hand side of each figure, the sum of the heats for the products is presented on the right-hand side, and the transition-state energies for each reaction are plotted in the middle.

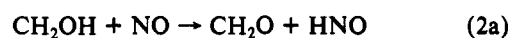
**CH<sub>2</sub>OH and CH<sub>2</sub>OH.** It is known that reaction of CH<sub>2</sub>OH with itself is fast. The figures illustrate that, indeed, a negative activation energy precedes the transition state for the mutual reaction



The general experience is that raising the temperature of a reaction leads to an increase in the specific rate constants describing the reaction. Occasionally, such as in reaction 1, the opposite behavior is encountered whereby when the temperature is increased the reaction slows down. This behavior can be understood by taking a closer look at the meaning of activation energy.<sup>22</sup> It can be shown that the experimental activation energy is simply the difference between the average energy of reacting molecules and the average energy of molecules in the system,<sup>22</sup>  $E_A = \langle E \rangle_{\text{reacting}} - \langle E \rangle_{\text{nonreacting}}$ . This implies that the reacting hydroxymethyl radicals have less internal thermal energy than the product HOCH<sub>2</sub>CH<sub>2</sub>OH molecules. The negative activation energy, calculated from the transition-state structure of reaction 1, means that the rate of combination is higher for those radicals with less than average thermal energy. As the temperature is raised, the population of radicals with less than average thermal energy is decreased and the effective rate of combination decreases with it.<sup>22</sup>

Table II summarizes the activation energy barriers and net energy requirements depicted in the figures. As can be seen for the CH<sub>2</sub>OH/CH<sub>2</sub>OH system, the activation energy for reaction 1 is -57.3 and -50.6 kcal/mol for the AM1 and PM3 calculations, respectively. The overall energy output from this exothermic reaction is predicted to be 58.3 and 51.0 kcal/mol by these two methods.

**CH<sub>2</sub>OH and NO.** In order to measure the kinetics of reactions of CH<sub>2</sub>OH with targets other than itself, Pagsberg et al.<sup>9</sup> used two different methods of analysis in order to account for reaction 1 and calculate a rate constant of  $2.5 \times 10^{-11}$  cm<sup>3</sup> molecule<sup>-1</sup> s<sup>-1</sup> for reaction 2. They propose that this rate constant consists of a combination of the rate constants for the abstraction reactions 2a and the addition reaction 2b.



We have also considered the corresponding abstraction/addition reactions where the oxygen atom of nitric oxide is the attacking atom

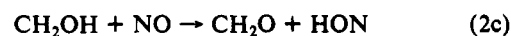
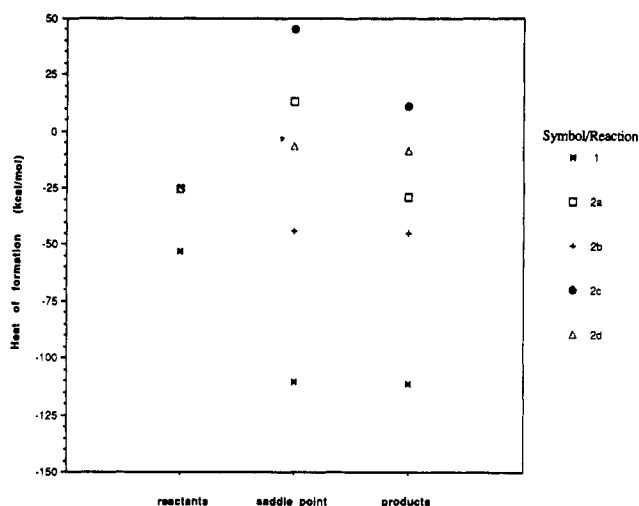


Table I illustrates that HNO is more stable than HON and HOCH<sub>2</sub>NO is more stable than HOCH<sub>2</sub>ON. Figure 1 displays the AM1 results from Tables I and II while Figure 2 displays the

(21) Benson, S. W.; Buss, J. H. *J. Chem. Phys.* **1958**, *29*, 546.

(22) Benson, S. W. *Thermochemical Kinetics*; John Wiley & Sons: New York, 1976.



**Figure 1.** AM1 heats of formation for reactants, products, and transition states for the  $\text{CH}_2\text{OH}/\text{NO}$  system. The sum of the calculated heats of formation for the reactants are plotted on the left, the sum of the heats of the products are plotted on the right, and the transition-state energy is plotted in the middle.

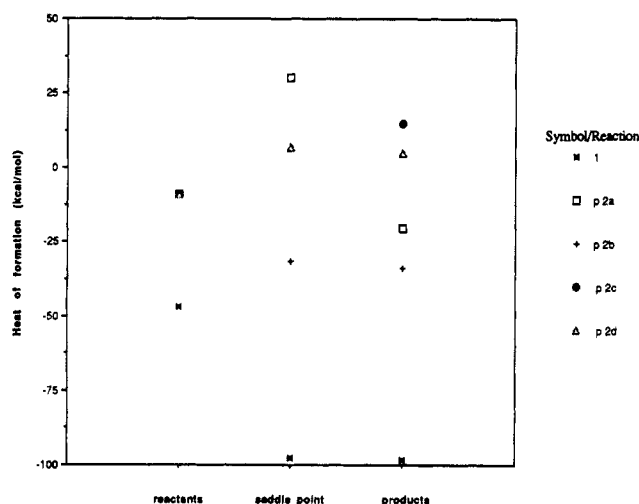
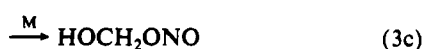
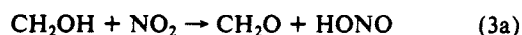


**Figure 2.** PM3 heats of formation for reactants, products, and transition states for the  $\text{CH}_2\text{OH}/\text{NO}$  system. The sum of the calculated heats of formation for the reactants are plotted on the left, the sum of the heats of the products are plotted on the right, and the transition-state energy is plotted in the middle.

PM3 results. The figures show that the addition reaction 2b is exothermic by approximately 20–25 kcal/mol and has a negative activation energy of roughly 20 kcal/mol. Reaction 2a is slightly exothermic but requires an activation energy of 38 kcal/mol to occur. An activation barrier of 15–19 kcal/mol is required for reaction 2d to occur, while reaction 2c is least likely to occur at room temperature. Numerical results from Figures 1 and 2 are listed in Table II. These findings lend support to the suggestion that the adduct product  $\text{HOCH}_2\text{NO}$  accounts for the residual ultraviolet spectrum in the pulse radiolysis experiment.<sup>9</sup> Reaction 2d, producing the adduct product  $\text{HOCH}_2\text{ON}$ , is the next most likely reaction to occur in this system.

**$\text{CH}_2\text{OH}$  and  $\text{NO}_2$ .** It has been proposed<sup>9</sup> that reactions of the hydroxymethyl radical with nitrogen dioxide which account for the measured rate constant of  $2.3 \times 10^{-11}$  are



In addition to these reactions, the reaction

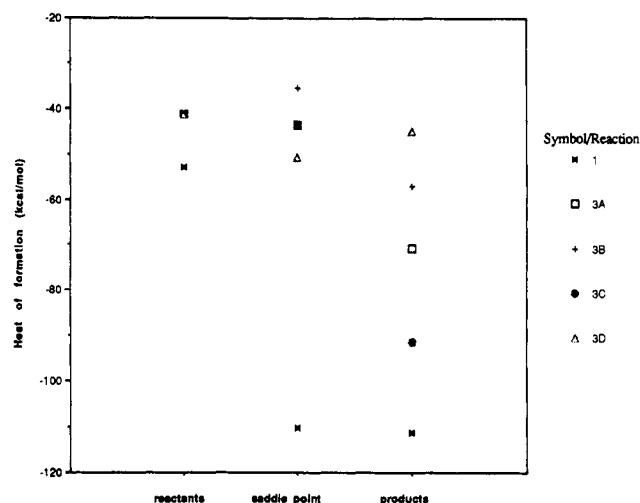
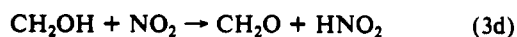


**Figure 3.** AM1 heats of formation for reactants, products, and transition states for the  $\text{CH}_2\text{OH}/\text{NO}_2$  system. The sum of the calculated heats of formation for the reactants are plotted on the left, the sum of the heats of the products are plotted on the right, and the transition-state energy is plotted in the middle.

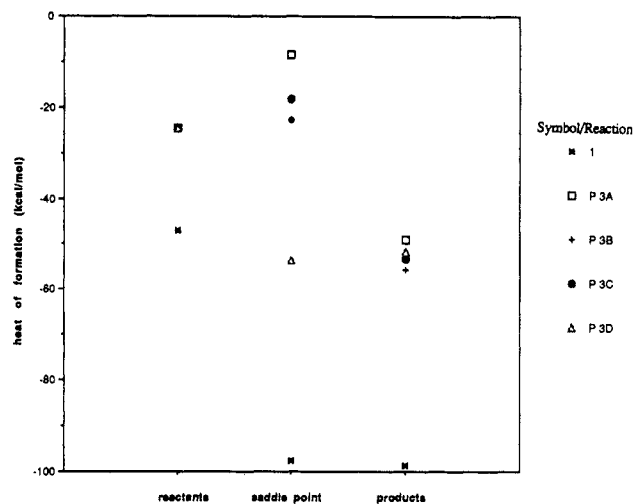


**Figure 4.** PM3 heats of formation for reactants, products, and transition states for the  $\text{CH}_2\text{OH}/\text{NO}_2$  system. The sum of the calculated heats of formation for the reactants are plotted on the left, the sum of the heats of the products are plotted on the right, and the transition-state energy is plotted in the middle.

is considered in this work. Table I shows that nitrous acid, a product in reaction 3a, is more stable than  $\text{HNO}_2$  by the AM1 calculations but a little less stable by PM3. The experimental heat of formation for  $\text{HONO}$  agrees well with the PM3 value. The adduct product  $\text{HOCH}_2\text{ONO}$  is again more stable than  $\text{HOCH}_2\text{NO}_2$  by AM1 but has about the same stability by the PM3 method. The energetics in Table I and II are displayed pictorially in Figures 3 and 4 for the AM1 and PM3 calculations, respectively. Figure 3 illustrates that reactions 3a, 3c, and 3d have negative activation energies. Reaction 3b has an activation energy of just 5 kcal/mol. All four reactions are exothermic. Figure 4 shows the results of the PM3 calculations. In this case, only reaction 3d has a negative activation energy, while reactions 3b and 3c require 2 and 6 kcal/mol for activation. It is of interest to note that reaction 3a to produce nitrous acid is least likely to occur according to the PM3 calculations. The energies depicted in Figures 3 and 4 are also summarized in Table II.

Much of the discrepancy between the AM1 and PM3 calculations is a consequence of the differences in calculated heats of formation for  $\text{NO}_2$  and  $\text{HONO}$ . For instance, the reactants  $\text{CH}_2\text{OH}$  and  $\text{NO}_2$  have a combined heat of formation of -41.5 kcal/mol when calculated by the AM1 method, but only -24.5 by PM3. This difference stems mainly from the calculated heat for  $\text{NO}_2$ , which is -15 kcal/mol for AM1 and -1 kcal/mol for

PM3. The experimental heat of formation for  $\text{NO}_2$  of 7.9 kcal/mol is closest to the PM3 value. For reaction 3a, not only is the value of the sums of the heats of formation for the reactants off by 17 kcal/mol but also the sum of the heats of formation for the products is off by approximately 22 kcal/mol. This product difference stems from the difference in the heat of formation for nitrous acid. As listed in Table I, the experimental heat of formation for HONO is -18.8 kcal/mol, which compares favorably with the PM3 value of -14.9 kcal/mol.

The new parametrization routine used to produce the PM3 Hamiltonian has been shown to be more accurate than the previous semiempirical methods for many different types of molecules.<sup>14</sup> Our findings for the  $\text{CH}_2\text{OH}$  system support this conclusion. Evaluating the results of the transition-state energies is more difficult as experimental information for activation barriers is not readily available. However, the information presented in Figures 3 and 4 allow us to describe an experiment that may help determine which method has correctly predicted the activation barriers. If the kinetics experiments were repeated at lower temperatures, insight could be gained on the behavior of the  $\text{CH}_2\text{OH}$  system. If the  $\text{CH}_2\text{OH}/\text{NO}_2$  system is described most accurately by the PM3 calculations outlined in Figure 4, then lowering the temperature should decrease the rate constant as reactions 3a, 3b, and 3c would contribute less and less at lower temperatures. On the other hand, Figure 3 shows that three of the four reactions have negative activation energies. Lowering

the temperature in this case should not decrease the rate constant in the same manner as in the PM3 case.

This same experimental technique of measuring rate constants at lower temperatures can also be used for the NO system. In this case, such experimental measurements would show whether reaction 2b is indeed the dominant reaction in the system. If it is, then the rate constant will not decrease with lower temperatures and reactions 2a, 2c, and 2d will be shown to have a small contribution to the overall rate constant.

### Conclusion

The AM1 and PM3 molecular orbital methods have been utilized to investigate the reactions of  $\text{CH}_2\text{OH}$  with NO and  $\text{NO}_2$ . For ground-state structures the PM3 method is superior for these systems. Both AM1 and PM3 predict that the dominant reaction of  $\text{CH}_2\text{OH}$  with NO produces the adduct  $\text{HOCH}_2\text{NO}$ , supporting the hypothesis from the pulse radiolysis/kinetic analysis experiments.<sup>9</sup> For the  $\text{NO}_2$  system the calculations predict the formation of  $\text{HOCH}_2\text{NO}_2$  and  $\text{HOCH}_2\text{ONO}$ . Furthermore, the PM3 calculations predict that formation of  $\text{CH}_2\text{O}$  and  $\text{HNO}_2$  is much more likely than the formation of  $\text{CH}_2\text{O}$  and HONO from reactions of the hydroxymethyl radical with nitrogen dioxide.

**Acknowledgment.** We thank Jim Oddo for technical assistance. This work was supported by a Bristol-Myers Co. Grant of Research Corporation.

## Ab Initio Molecular Orbital Study of Adducts and Oxides of Boron Hydrides

Gilbert J. Mains

Department of Chemistry, Oklahoma State University, Stillwater, Oklahoma 74078  
(Received: October 12, 1990)

Ab initio molecular orbital theory at the HF/6-31G\* level has been used to investigate the structures of Lewis acid/base adducts of boron hydrides with argon and a variety of substrates that may be encountered in the mechanism for the oxidation of diborane. By use of fourth-order Møller-Plesset theory, i.e., MP4SDTQ, correlation effects are calculated at the HF/6-31G\* geometries. Borane was found to form stable adducts with dioxygen, hydroxyl radical,  $\text{O}(^3\text{P})$  atom, and  $\text{H}-\text{B}=\text{O}$ . Structures of isomeric forms of  $\text{HBO}$ ,  $\text{H}_2\text{BO}$ ,  $\text{H}_3\text{BO}$ ,  $\text{H}_3\text{BO}_2$ ,  $\text{H}_3\text{B}_2\text{OH}$ ,  $\text{H}_4\text{B}_2(\text{OH})_2$ ,  $\text{H}_5\text{B}_2\text{O}$ ,  $\text{H}_5\text{B}_2\text{O}_2$ ,  $\text{H}_4\text{B}_2\text{O}$ , and cyclic  $(\text{HBO})_3$  were investigated. Evidence is presented for Lewis acid/base adducts with  $\text{BH}_2$  radical and some oxygenated boranes. The number and stability of these adducts suggest that the mechanism of the oxidation of diborane is much more complicated than that of ethane where adduct formation can be neglected.

### Introduction

Borane chemistry is very rich and much studied. Since boron has only five electrons, early theoretical studies focused on simple boron hydrides,  $\text{BH}$ ,  $\text{BH}_2$ , and  $\text{BH}_3$ , because these could be studied with the available computational facilities. The development of more sophisticated computers permitted treatment of molecules with more electrons, e.g., the adducts of  $\text{BH}_3$  with CO and  $\text{NH}_3$ , and diborane itself was examined. Diborane,  $\text{H}_2\text{B}(\mu\text{-H})_2\text{BH}_2$ , is the prototype structure for  $\mu$ -hydrido bridging in electron-deficient systems. Consequently, the structural and electronic properties of this novel dimer have been studied extensively, both experimentally and computationally. A recent review has been published.<sup>1</sup> Ab initio techniques are being used to unravel the complex kinetics of diborane pyrolysis,<sup>2</sup> although the rate-determining step is still in doubt.<sup>3</sup> Recent studies have found that the  $\text{BH}_3\cdots\text{H}_2$

adduct<sup>4</sup> is remarkably stable and that correlation effects are very important in determining the structure of triborane.<sup>5</sup>

On the other hand, much less is known about the oxidation of boranes, although that of diborane has been the subject of several experimental studies.<sup>6-9</sup> Modeling of the oxidation has been recommended<sup>10</sup> and used by Borchardt et al.<sup>9</sup> to reproduce the OH radical profile generated by the reaction of  $\text{O}(^3\text{P})$  atoms with diborane. This modeling was performed before it was recognized that the  $\text{B}_2\text{H}_5$  radical could exist in isomeric forms<sup>11-13</sup> and the

(1) Liebman, J. F.; Greenberg, A.; Williams, R. E., Eds. *Advances in Boron and Boranes*; VCH Publishers: New York, 1988.

(2) Stanton, J. F.; Lipscomb, W. N.; Bartlett, R. J. *J. Am. Chem. Soc.* **1989**, *111*, 5165.

(3) Greaux, R.; Greenwood, N. N.; Lucas, S. M. *J. Am. Chem. Soc.* **1989**, *111*, 8721.

(4) Stanton, J. F.; Lipscomb, W. N.; Bartlett, R. J. *J. Am. Chem. Soc.* **1989**, *111*, 5173.

(5) Stanton, J. F.; Lipscomb, W. N.; Bartlett, R. J.; McKee, M. L. *Inorg. Chem.* **1989**, *28*, 109.

(6) Carabine, M. D.; Norrish, R. G. W. *Proc. R. Soc. (London)* **1967**, *296*, 1.

(7) Hand, C.; Derr, L. K. *Inorg. Chem.* **1974**, *13*, 339.

(8) Jeffers, P. M.; Bauser, S. H. *J. Phys. Chem.* **1984**, *88*, 5039.

(9) Borchardt, D. B.; Choi, G.-G.; Suzuki, K.; Bauer, S. H. *J. Chem. Phys.* **1988**, *88*, 6282.

(10) Shaub, W. M.; Lin, M. C. *Natl. Bur. Stand. (U.S.) Spec. Publ.* **561** **1979**, 1249.

(11) Mains, G. J.; Bock, C. W.; Niki, H.; Trachtman, M. *Struct. Chem.* **1990**, *1*, 171.

(12) Curtiss, L.; Pople, J. A. *J. Chem. Phys.* **1989**, *91*, 4183.